Study on the structure of Fe/MgO catalysts for H_2S wet oxidation

Kwang-Deog Jung *, Oh-Shim Joo and Chul-Sung Kim [a]

Eco-Nano Center, Korea Institute of Science and Technology, P.O. Box 131, Seoul, Korea
[a] Department of Physics, Kookmin University, Seoul 136-702, Korea

Received 7 May 2002; accepted 7 August 2002

Wet catalytic oxidation was performed at room temperature with 1 wt% Fe/MgO, 4 wt% Fe/MgO, 6 wt% Fe/MgO, 15 wt%/MgO and 30 wt% Fe/MgO catalysts. The 6 wt% Fe/MgO catalyst has a maximum capacity of 2.6 g H_2S/g_{cat} for H_2S removal. The amounts of paramagnetic Fe^{3+} cations are correlated with the H_2S removal capacity of the Fe/MgO catalysts from Mössbauer experiments. It is observed that the deactivation of the 6 wt% Fe/MgO catalyst can be due to the loss of the paramagnetic Fe^{3+} cations during the reaction.

KEY WORDS: wet oxidation; H_2S removal; Fe/MgO catalyst; Mössbauer.

1. Introduction

The iron oxide or iron sponge process is one of the oldest gas-treating processes still in use, since iron oxide catalyst has been used to catalyze the selective oxidation of hydrogen sulfide to elementary sulfur [1,2]. The Superclaus process was first developed to obtain an H_2S removal efficiency of 99.5% at a temperature of around 513 K on Fe–Cr/Al_2O_3 or Fe/SiO2 [3] and the BSR/Selectox process on Fe/Al_2O_3 reaches the same performance [4]. The total oxidation of H_2S to SO_2 could not be avoided at a temperature above the sulfur dew point. The Doxosulfreen process is conducted at a temperature below 413 K for suppressing the large total oxidation of H_2S to SO_2 [5,6]. Nonetheless, the reaction temperature is too high to prevent the SO_2 and metal sulfide formation. The H_2S oxidation at a temperature below 373 K has rarely been attempted on metal oxides, but it has extensively been studied on carbons. Recently, it was reported that carbons as a catalyst could be capable of sorbing 0.66 g of sulfur/g carbon [7]. However, the catalytic system required the chemicals to control the pH of an aqueous solution. In this study, an Fe/MgO catalyst is optimized to have a high activity for H_2S oxidation at room temperature. The H_2S removal capacity of Fe/MgO catalysts is correlated with the paramagnetic iron content in Fe/MgO.

2. Experimental

Fe/MgO catalysts were prepared by an impregnation of MgO (Aldrich 22,036-1) with aqueous iron nitrate solutions, followed by drying at 373 K and subsequent calcination in air for 5 h at 733 K. Fe/MgO catalysts (1 wt%, 4 wt%, 6 wt%, 15 wt%, and 30 wt% Fe/MgO) were prepared with changing iron concentrations. The samples were designated as Fe (weight percentage)/MgO. The base-treated activated carbon (TSX, Dongyang Carbons) and the physically mixed Fe(6)/MgO catalyst are used for the activity comparison with the Fe(6)/MgO catalyst. The physically mixed Fe(6)/MgO sample was prepared by grinding Fe_2O_3 (Aldrich 20,351-3) with MgO (Aldrich 22,036-1). The activity measurements were carried out using a stirred batch tank reactor. The catalyst samples (3.0 g) were dispersed in the reactor charged with distilled water (1.5 L), and the reactant gases were supplied through a perforated rubber plate at the bottom of the reactor. The reactants were stirred with a mechanical stirrer. H_2S concentrations from the reactor were measured with on-line G.C. with an FPD detector which can detect up to 0.1 ppm H_2S. A Porapak Q column ($\frac{1}{8}$ in. (O.D.) × 2 m) was used for separating the product gases.

Mössbauer spectra were recorded using a conventional Mössbauer spectrometer of the electromechanical type with a 30 mCi ^{57}Co source in an Rh matrix.

X-ray photoelectron spectra were obtained using Al K_α radiation (Phi 5800, Physical Electronics). The surface areas of the Fe/MgO catalysts were measured with an ASAP 2000 (Micromeritics).

3. Results and discussion

Figure 1 shows the H_2S removal behavior of the Fe(6)/MgO catalyst. The base-treated activated carbon (TSX) and the physically mixed Fe(6)/MgO were used for comparison. In these experiments, feed gases (H_2S: 5 mL/min, O_2: 100 mL/min) were introduced into the stirred slurry reactor with 1.5 L of distilled water and

* To whom correspondence should be addressed.
E-mail: jkdcat@kist.re.kr

1011-372X/02/1100-0053/0

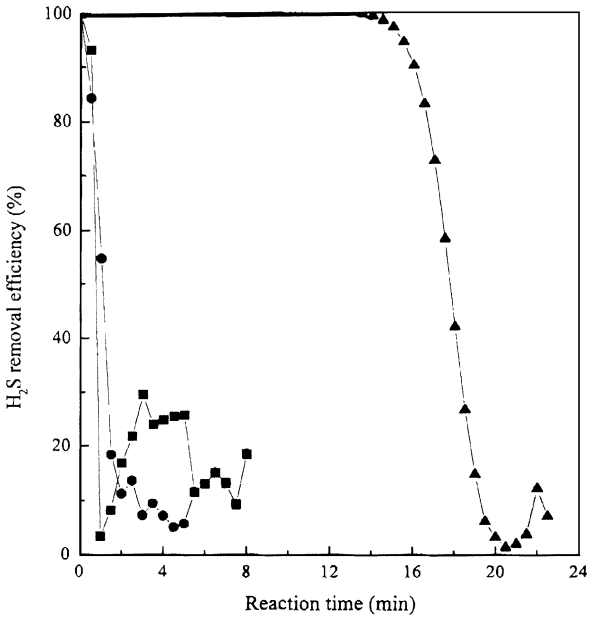

Figure 1. Wet oxidation of H_2S to sulfur at room temperature on the activated carbon (■), the physically mixed Fe(6)/MgO (●) and the Fe(6)/MgO (▲).

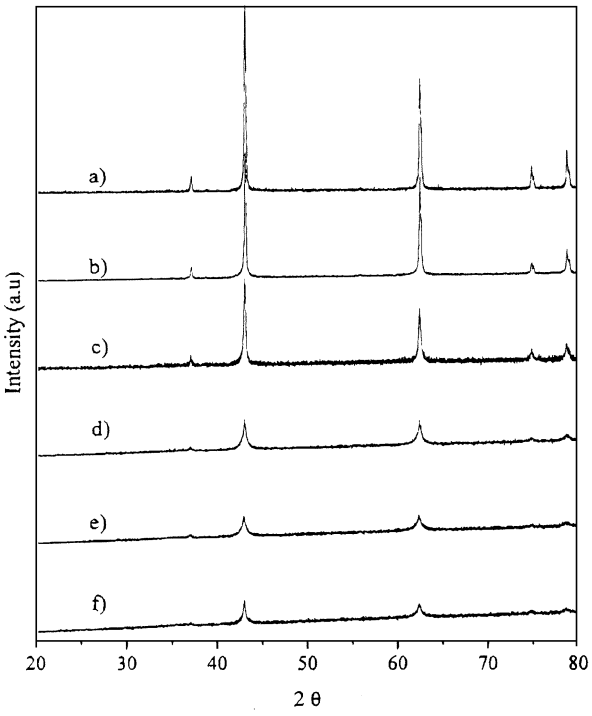

Figure 2. X-ray diffractograms of (a) MgO, (b) Fe(1)/MgO, (c) Fe(4)/MgO, (d) Fe(6)/MgO, (e) Fe(15)/MgO, (f) Fe(30)/MgO.

3 g of catalyst. The wet oxidation experiments at room temperature show the breakthrough curve for H_2S removal. Both the activated carbon and the physically mixed Fe(6)/MgO have an H_2S removal capacity of 0.10–0.15 g H_2S/g_{cat}, while the Fe(6)/MgO have a removal capacity of 2.6 gH_2S/g_{cat}. The H_2S removal capacity was obtained by calculating the total amount of H_2S removed up to 50% of the H_2S removal efficiency. The higher H_2S removal capacity of Fe(6)/MgO as compared to that of the physically mixed Fe_2O_3(6)/MgO indicates that the physical adsorption should not be important for H_2S removal. For further investigation of the catalytic behavior of the Fe/MgO, the effects of the iron concentrations in Fe/MgO were examined for the H_2S removal.

Table 1 shows the H_2S removal capacity of Fe(1)/MgO, Fe(4)/MgO, Fe(6)/MgO, Fe(15)/MgO and Fe(30)/MgO. The H_2S removal capacity of the Fe(4)/MgO is nearly four times higher than that of the Fe(1)/MgO, meaning that the removal capacity of the Fe/MgO is proportional to the iron concentrations in the Fe/MgO. Here, it is interesting to note that the H_2S removal capacity is maximized with the Fe(6)/MgO. The Fe(15)/MgO and the Fe(30)/MgO have lower H_2S removal capacity than the Fe(6)/MgO. The iron concentration dependencies on the H_2S removal capacity support the idea that H_2S can be removed by a catalytic reaction and suggest that the iron component should be responsible for the H_2S oxidation reaction at room temperature.

Figure 2 shows X-ray diffractograms of Fe/MgO samples. Interestingly, no iron oxide characteristic peaks appear even with Fe(30)/MgO and MgO intensity decreases with the iron concentrations. The absence of the iron oxide characteristic peaks indicates that iron components are well dispersed in MgO. It was observed that MgO was dissolved when an aqueous iron nitrate solution ($pH \approx 1$) was added into the MgO slurry for the catalyst preparation. After a few minutes, a paste-like solid was formed near $pH = 7$ of the solution, since the dissolved MgO increased the pH of the solution to co-precipitate with the iron component. This preparation procedure can explain the absence of iron oxide characteristic peaks and the decrease of MgO intensity with the iron concentration in the Fe/MgO catalysts.

Figures 3 and 4 show the Mössbauer spectra of the Fe/MgO catalysts at 293 K and 13 K, respectively. Table 2

Table 1
The H_2S removal capacity of the Fe/MgO catalysts.

Catalysts	Fe(1)/MgO	Fe(4)/MgO	Fe(6)/MgO	Fe(15)/MgO	Fe(30)/MgO
The H_2S removal capacity, g H_2S/g_{cat}	0.6	2.2	2.6	2.4	1.7

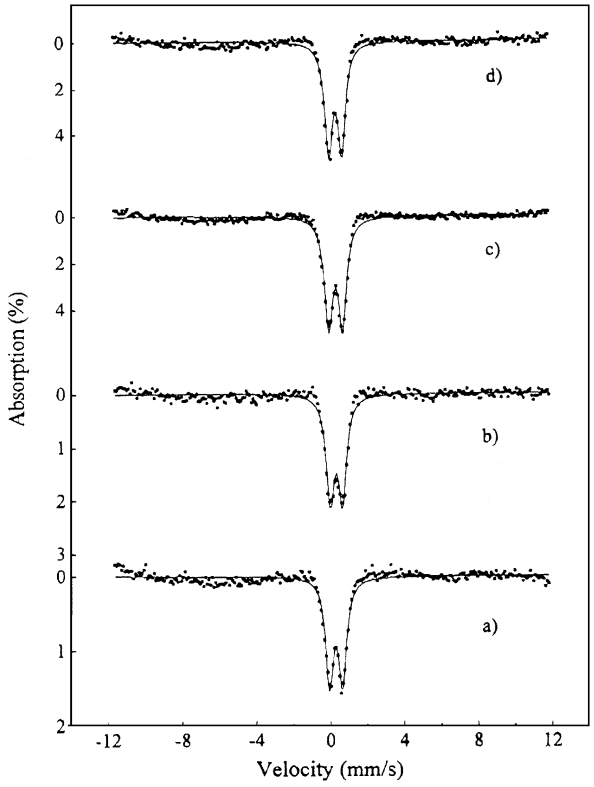

Figure 3. Mössbauer spectra at 293 K of (a) Fe(4)/MgO, (b) Fe(6)/MgO, (c) Fe(15)/MgO, (d) Fe(30)/MgO.

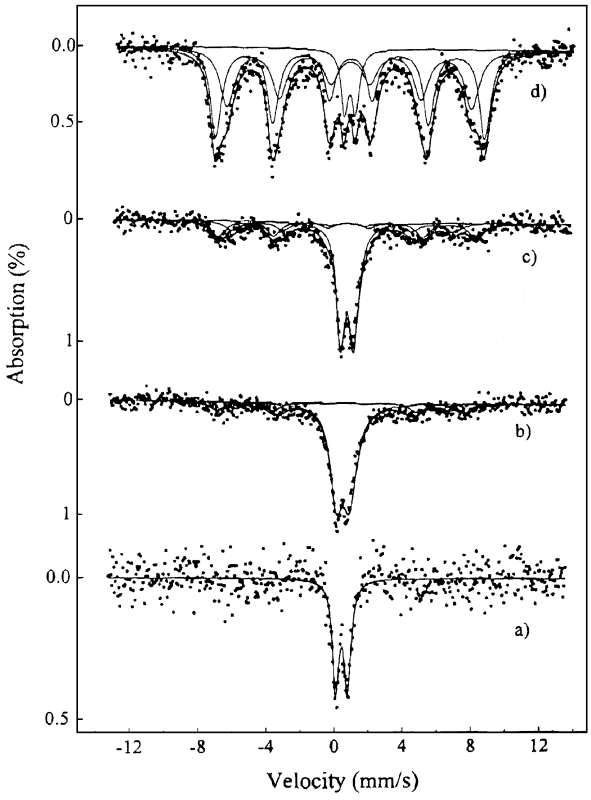

Figure 4. Mössbauer spectra at 13 K of (a) Fe(4)/MgO, (b) Fe(6)/MgO, (c) Fe(15)/MgO, (d) Fe(30)/MgO.

shows the Mössbauer parameters of Fe/MgO catalysts.

The doublet (2 line) of the Fe/MgO catalysts at 293 K may be due to very small particles showing super-paramagnetic relaxation, or paramagnetic Fe^{3+} cations [8–10]. Both doublets at 293 K and 13 K can be assigned to the presence of the paramagnetic Fe^{3+} cations [8]. The Mössbauer spectra of the Fe(4)/MgO show only the doublet even at 13 K. The sextets (6 line) at 13 K start to appear from the Fe(6)/MgO and the proportions of the sextets increase with iron concentrations in Fe/MgO, indicating that the super-paramagnetic iron oxide particles and the paramagnetic Fe^{3+} cations coexist in the Fe/MgO samples with an iron content above 6 wt%. The small particles of the sextets can be mainly attributed to the $MgFe_2O_4$ spinel from the observation of the A site (tetrahedral) and the B site (octahedral) [11], although the small proportion of the α-Fe_2O_3 presence cannot be ruled out. The hyperfine field of Fe(6)/MgO ($H = 386.1$ kOe for A site and $H = 454.0$ kOe for B site) are much smaller than that of pure α-Fe_2O_3 (*ca* 525 kOe) and that of $MgFe_2O_4$ ($H = 511$ kOe for A site and $H = 538$ kOe for B site at 75 K).

Table 2
Mössbauer parameters at 293 K and 13 K of the Fe/MgO catalysts.

Samples	6 line–2 set						2 line–1 set		Area (%)	
	H_{hf} (kOe)		E_Q (mm/s)		δ (mm/s)		E_Q (mm/s)	δ (mm/s)	6 line	2 line
	A	B	A	B	A	B				
Fe(4)/MgO at 298 K							0.70	0.26		100
Fe(6)/MgO at 298 K							0.65	0.27		100
Fe(15)/MgO at 298 K							0.74	0.27		100
Fe(30)/MgO at 298 K							0.70	0.27		100
Fe(4)/MgO at 14 K							0.69	0.40		100
Fe(6)/MgO at 14 K	386	454	−0.04	−0.10	0.31	0.33	0.77	0.39	24.5	75.5
Fe(15)/MgO at 14 K	403	469	−0.05	−0.01	0.14	0.37	0.63	0.41	56.0	44.0
Fe(30)/MgO at 14 K	446	491	−0.02	−0.05	0.37	0.43	0.64	0.38	91.1	8.9

Table 3
Area of the paramagnetic Fe^{3+} cations of the Fe/MgO samples.

Catalysts	BET area (m^2/g)	Atomic iron percentage by XPS, Fe/(Fe + Mg) × 100 (%)	Doublet area of Mössbauer spectra (%)	Area of paramagnetic Fe^{3+} cations (m^2/g)
Fe(1)/MgO	30.7	–	–	–
Fe(4)/MgO	27.3	2.0	100.0	0.55
Fe(6)/MgO	49.4	2.5	75.5	0.93
Fe(15)/MgO	65.4	3.2	44.0	0.92
Fe(30)/MgO	45.0	7.1	8.9	0.28

The much lower hyperfine field of the Fe/MgO can be attributed to the small size of the $MgFe_2O_4$ particles or the iron particles. The hyperfine fields of Fe/MgO catalysts increase with iron content. This can be attributed to the increase of the magnetic order resulting from the increase of the particle size. The most reliable percentages of each species (doublets and sextets) can be estimated at low temperature, since the probable differences in the recoil-free factors are minimal. The total areas of iron component at the surface of the Fe/MgO catalysts are estimated by multiplying the atomic iron fraction at the surface, Fe/(Mg + Fe), by BET surface areas. The atomic iron fractions, Fe/(Fe + Mg), were measured by XPS. The atomic size of Fe^{3+} is assumed to be the same as that of Mg^{2+}, since the ionic radius of Mg^{2+} (86 nm) is not very different from that of Fe^{3+} (63–92 nm). Finally, the areas of the paramagnetic Fe^{3+} cations on Fe/MgO samples are calculated by multiplying the iron areas at the surface of the Fe/MgO catalysts by the relative areas (%) of the doublet of Mössbauer spectra. Table 3 shows the areas of the paramagnetic Fe^{3+} cations on the Fe/MgO catalysts.

As shown in table 3, the removal capacities of the Fe/MgO catalysts (table 1) are well correlated with the areas of paramagnetic Fe^{3+} cations, suggesting that the paramagnetic Fe^{3+} cations can be an active species for H_2S oxidation at room temperature. The paramagnetic Fe^{3+} cations can be regarded as the isolated Fe^{3+} cations in the MgO matrix [8].

Homogeneous catalysts (Fe^{3+}-chelating agent) have been used for H_2S oxidation by liquid redox processes [12–14]. In the reaction, Fe^{3+} cations were active species and several chelating agents were used for stabilizing Fe^{3+} cations. Similarly to the homogeneous catalysts, it is proposed that the isolated Fe^{3+} cations in Fe/MgO catalysts can be an active species in the H_2S oxidation at room temperature.

The catalysts are deactivated during the reaction, as shown in figure 1. The Mössbauer experiments were conducted to monitor the changes of the iron properties on the Fe(6)/MgO samples after 3 h, 6 h and 12 h reaction. Figure 5 and table 4 show the Mössbauer spectra and the Mössbauer parameters at 13 K of the used Fe(6)/MgO catalysts. The 2-line areas (%) of the used Fe(6)/MgO catalysts are 99.2, 84.8 and 12.4 after the reaction for 3 h, 6 h and 12 h, respectively. This means that the concentrations of the isolated Fe^{3+} cations in the Fe(6)/MgO decrease with the reaction time. The increase of the 6-line area (%) can result from the agglomeration of the paramagnetic Fe^{3+} cations during the reaction, even at room temperature.

It is plausible that the active species of the Fe(6)/MgO catalysts can steadily be lost during the reaction, although the H_2S removal efficiency starts to decrease after 12 h of reaction. Therefore, it is concluded that the deactivation of the Fe(6)/MgO catalyst can be due to the decrease of the isolated Fe^{3+} cations, supporting the isolated Fe^{3+} cations as the active species for the H_2S oxidation.

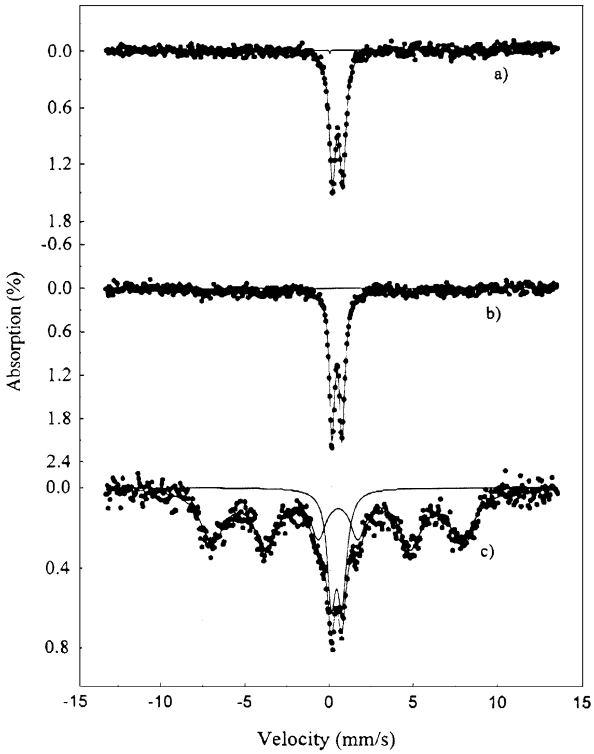

Figure 5. Mössbauer spectra of Fe(6)/MgO at 13 K after the reaction of (a) 3 h, (b) 6 h and (c) 12 h at room temperature.

Table 4
Mössbauer parameters of the Fe(6)/MgO at 13 K after 3 h, 6 h, 12 h reaction.

Fe(6)/MgO	6 line–1 set			2 line–1 set		Area (%)	
	H_{hf} (kOe)	E_Q (mm/s)	δ (mm/s)	E_Q (mm/s)	δ (mm/s)	6 line	2 line
After 3 h reaction	–	0.000	−0.119	0.61	0.33	0.8	99.2
After 6 h reaction	463	−0.05	0.57	0.60	0.34	15.2	84.8
After 12 h reaction	461	−0.03	0.44	0.63	0.31	87.6	12.4

4. Conclusions

Fe/MgO catalysts are shown to be effective for the H_2S removal. The amounts of paramagnetic Fe^{3+} cations on Fe/MgO are correlated with the H_2S removal capacities, indicating that the paramagnetic Fe^{3+} cations can be active species for H_2S oxidation. The concentrations of the paramagnetic Fe^{3+} cations of the Fe(6)/MgO decrease with the reaction time. It can be concluded that the deactivation of the Fe/MgO catalysts can be due to the decrease of the paramagnetic Fe^{3+} cations, *i.e.*, the agglomeration of the paramagnetic Fe^{3+} cations.

References

[1] C.D. Swaim, Jr., Hydrocarbon Process 49(3) (1970) 127.
[2] R.N. Maddox and M.D. Burns, Oil & Gas J. June (1968) 90.
[3] P.F.M.T. van Nisselroony and J.A. Lagas, Catal. Today 16 (1993) 263.
[4] Parsons, Sulfur, 250 (1977) 60.
[5] S. Savin, O. Legendre, J.B. Nougayrede and C. Nedez, Sulfur 296 (1998) 523.
[6] S. Savin, J.B. Nougayrede, W. Willing and G. Brandel, Int. J. Hydrocarbon Eng. (1998) 2241.
[7] A.K. Dalai, A. Majumdar and E.L. Tollefson, Environ. Sci. Technol. 33 (1999) 54.
[8] R. Spretz, S.G. Marchetti, M.A. Ulla and E.A. Lomburdo, J. Catal. 194 (2000) 167.
[9] K. Chen, Y. Fan, Z. Hu and Q. Yan, J. Mater. Chem. 6(6) (1996) 1041.
[10] K. Chen, Y. Fan, Z. Hu and Q. Yan, J. Solid State Chem. 121 (1966) 240.
[11] E. De Grave, A. Grvaert, D. Chambaere and G. Robbrecht, Physica 96B (1979) 103.
[12] L.C. Hardison, AICHE Spring National Meeting, New Orleans, 2 April 1993.
[13] D.W. Newman and S. Lynn, Am. Inst. Chem. Eng. J., 30(1) (1984) 62.
[14] D.A. Dalrymple, T.W. Trofe and D. Leppin, Oil & Gas J. May (1994) 54.